Journal of Hydrology (2006) 329, 724–729

available at www.sciencedirect.com

ScienceDirect

journal homepage: www.elsevier.com/locate/jhydrol

DISCUSSION

Comment on ''Using numerical modelling to evaluate the capillary fringe groundwater ridging hypothesis of streamflow generation'' by H. L. Cloke, et al. [J. Hydrol. 316 (2006) 141–162]

Jozsef Szilagyi *

Department of Hydraulic and Water Resources Engineering, Budapest University of Technology and Economics, 1111 Muegyetem Rkp. 3-9, Budapest, Hungary
[1] *Conservation and Survey Division, University of Nebraska—Lincoln, 113 Nebraska Hall, Lincoln, NE 68588-0517, USA*

Received 19 January 2006; accepted 23 March 2006

Cloke et al. (2006) discuss an interesting topic of runoff generation, a central theme in hydrology. While their numerical experiment reproduced the physical experiment of Abdul and Gillham (1984) with good agreement, I feel that their proposed generalization of the model results to more realistic natural settings of riparian zones is not perfectly well supported. This is so because the stream channel initially is disconnected from the groundwater in Abdul and Gillham (1984) experiment which is replicated by Cloke et al. (2006) (Figs. 2, 4, and 6) in their above numerical study. In my opinion the initially disconnected stream setting ought to be replaced by a more common (at least in humid climates) perennially gaining stream example where groundwater is in continuous contact with the channel through the stream-aquifer interface permitting immediate water fluxes across it when responding to precipitation. This more realistic boundary condition at the stream-aquifer interface will allow rapid groundwater inflow to the stream and should be taken into consideration when commenting upon the role of groundwater ridging in runoff generation. Below such a numerical experiment is described and the results subsequently discussed.

The computational domain, representing the aquifer, is displayed in Fig. 1. As is seen, the aquifer has a gently sloping ground surface (slope is 1%) and an also, similarly sloping impermeable layer at the bottom. Initially ($t = 0$), it contains a horizontal groundwater-table at $y = 0.1$ m (Fig. 2), representing a static equilibrium, i.e., hydraulic head (h) is constant everywhere. The aquifer is drained for $t > 0$ by an instantaneous drop in the stage (i.e. from 0.1 m at $t = 0$ to 0 m for $t > 0$) of the fully penetrating stream on the right side. Note that a full or partial penetration of the stream is not of a fundamental difference in many cases. If the stream channel is deep and narrow and/or when its bottom is made up of clayey deposits, stream aquifer interactions across the channel bottom may be limited compared to water exchanges along the channel sides, especially for incised streams.

Precipitation (P) will arrive at the ground surface with intensities that follow a squared sine-curve for a half-period (Fig. 3)

$$P = 0.14K_s \sin^2(5.102t), \tag{1}$$

* Corresponding author. Address: Conservation and Survey Division, University of Nebraska—Lincoln, 113 Nebraska Hall, Lincoln, NE 68588-0517, USA.
E-mail address: jszilagyi1@unl.edu.
[1] A contribution of the University of Nebraska Agricultural Research Division, Lincoln, NE 68583, USA. Journal Series Number 15091.

0022-1694/$ - see front matter
doi:10.1016/j.jhydrol.2006.03.020

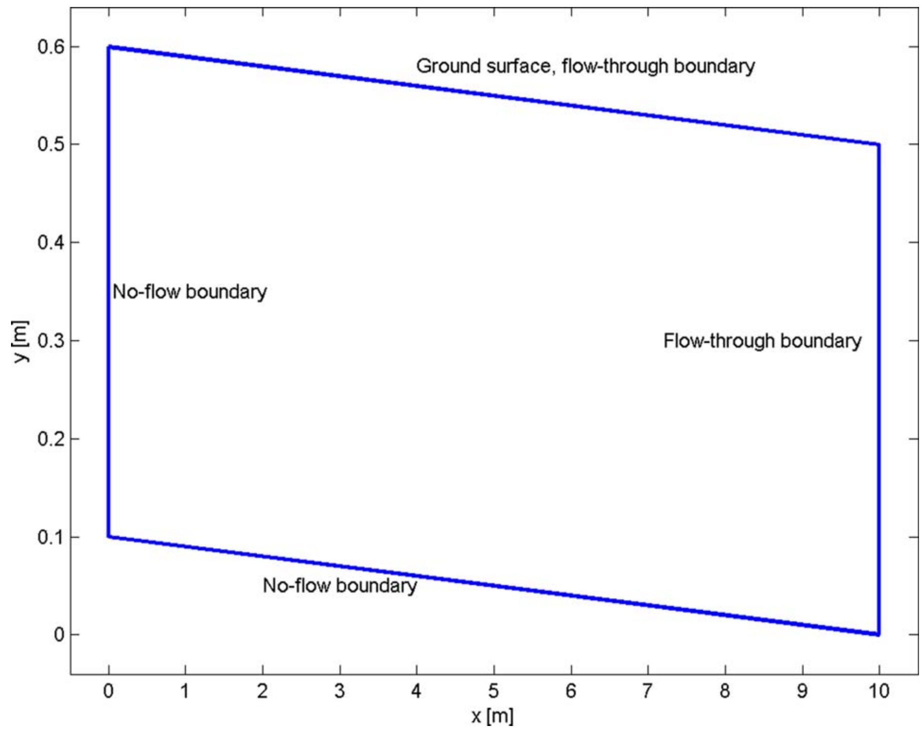

Figure 1 The computational domain and the boundary conditions applied for a gently sloping aquifer.

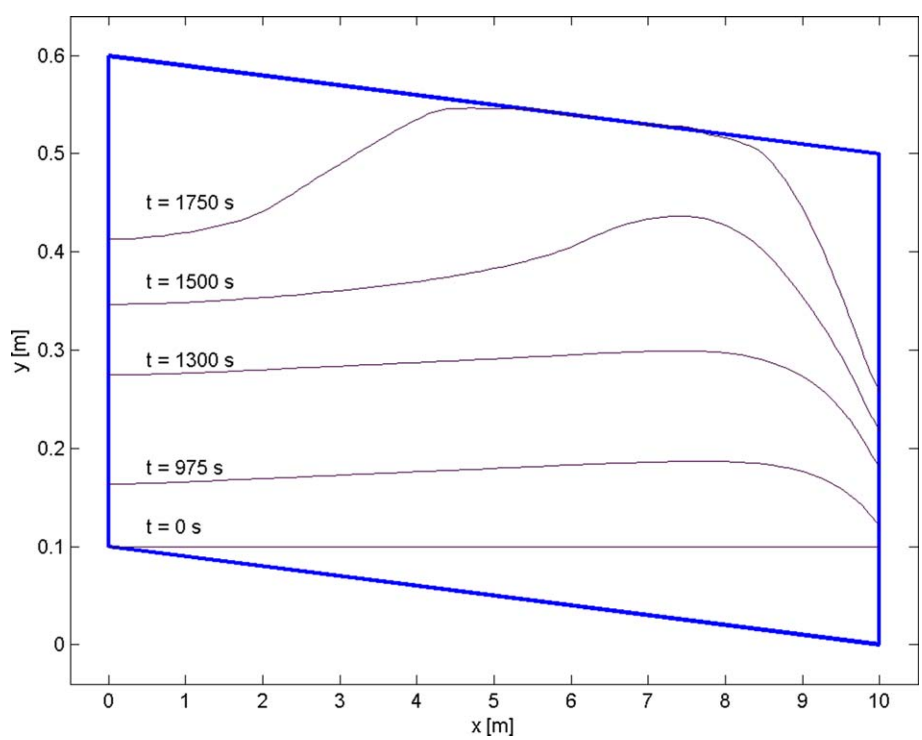

Figure 2 Evolution of the groundwater table through time.

where K_s is the saturated hydraulic conductivity of the assumed sand aquifer material, and t is measured in hours. See Szilagyi (2003) for the prescribed hydraulic properties of the aquifer material.

Aquifer drainage and recharge was simulated by a finite element model (Flexpde) that numerically integrates the combined unsaturated/saturated flow equation (Lam et al., 1987)

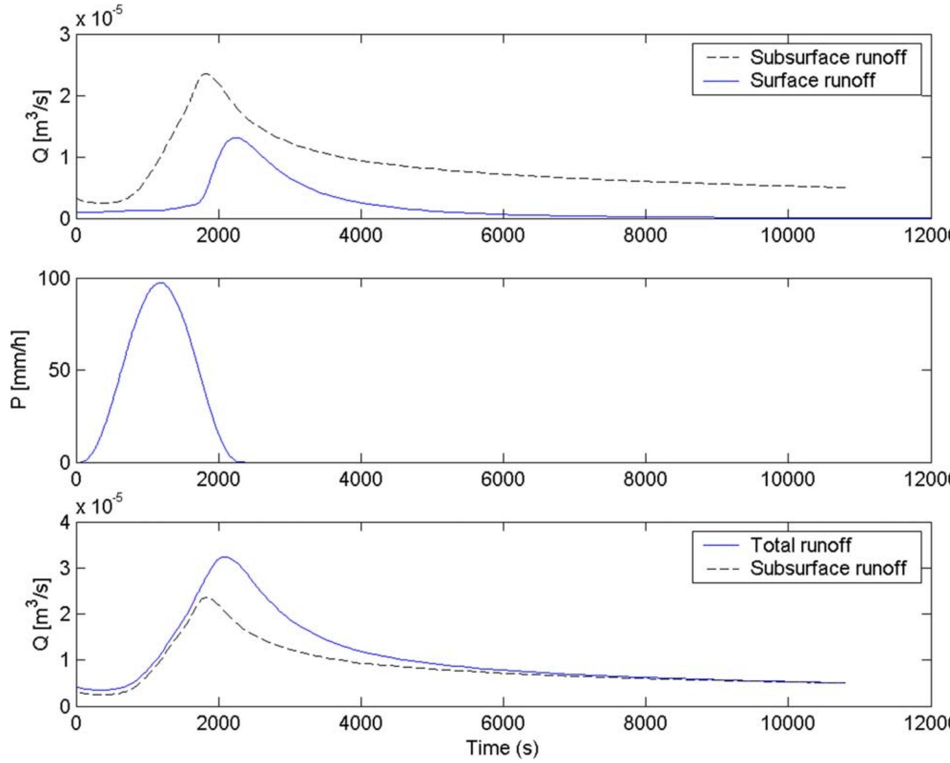

Figure 3 Rainfall hyetograph and the resulting surface, subsurface, and total runoff hydrographs of the gently sloping aquifer.

$$\frac{\partial}{\partial x}\left(K(\psi)\frac{\partial h}{\partial x}\right)+\frac{\partial}{\partial y}\left(K(\psi)\frac{\partial h}{\partial y}\right)=m\gamma\frac{\partial h}{\partial t} \qquad (2)$$

where K, a function of the suction/pressure head (ψ) here denotes both unsaturated and saturated hydraulic conductivities; m is the slope of the water–retention curve, which becomes the coefficient of volume change in the saturated zone (Lam et al., 1987); and γ is the unit weight of water.

On the right side of the domain a value boundary condition is evoked whenever the suction/pressure head, ψ, is positive, otherwise it is a no flow boundary. At the ground-surface water can enter the domain at the precipitation rate as long as ψ is negative. It becomes a value boundary otherwise (Gitirana et al., 2005).

The difference in precipitation intensity and infiltration (q) over the ground surface becomes as input (a function of time and position) of a separate surface runoff model. Surface runoff (Q) is modeled by the nonlinear kinematic wave equation (Berod et al., 1999) with an additional linear diffusion term for numerical stability

$$\frac{\partial Q}{\partial t}+c(Q)\frac{\partial Q}{\partial x}+D\frac{\partial^2 Q}{\partial x^2}=c(Q)q \qquad (3)$$

with a celerity term of $c(Q)=1.5(CS_0^{0.5})^{2/3}Q^{1/3}$. Here C is the Chezy roughness parameter, S_0 is the slope of the ground surface and D is a constant diffusion coefficient. A D value of 0.01 $m^2\,s^{-1}$ and a C value of 1 $m^{0.5}\,s^{-1}$ was employed in the model, this latter is of the same magnitude as the values cited by Berod et al. (1999) for prairie grass cover. With the above one-way coupling of the surface and subsurface runoff processes an implicit assumption is made that once water is available for surface runoff it stays on the surface until it reaches the stream, i.e. no subsequent infiltration is possible from this water flowing on the ground surface.

Fig. 2 displays the evolution of the groundwater-table elevations through time while in Fig. 3 the ensuing surface, subsurface, and total runoff hydrographs of the aquifer, having a unit length along the stream, can be seen. Comparing the two figures it becomes apparent that groundwater influx to the stream channel is well advanced by the time the groundwater table surfaces, thus the latter cannot be the cause of rapid and significant groundwater influx to the stream (i.e., baseflow). Since the aquifer in the model is made up of sand, the capillary fringe has a negligible thickness (see Szilagyi, 2003), thus its collapse cannot be the triggering mechanism either. As it is argued below, the real driving force behind the observed rapid groundwater influx to the stream is the necessary presence of sharp gradients in the hydraulic head near the stream bank, resulting in large Darcy-fluxes (Fig. 4), which is different from the requirement of a groundwater ridge. The groundwater ridge in Fig. 2 develops because the horizontal groundwater table initially is closer to the surface near the stream than farther away of it due to a sloping surface (Fig. 2). The vadose zone consequently retains more moisture near the stream initially and can become saturated faster during a rain event.

The following can be concluded from the present numerical study. If groundwater ridging is defined as the emergence of groundwater on the surface from saturation excess (Fig. 1 of Cloke et al. (2006)), then groundwater ridging is not the cause of fast and significant baseflow contribution to the stream in our example. Rather, it is the opposite, groundwater ridging blocks the infiltration of additional water into the soil-aquifer system, thus boosting surface runoff. A comparison of Figs. 2 and 3 demonstrates that surface runoff indeed intensifies when the groundwater table reaches the surface at around 1700–1800 s.

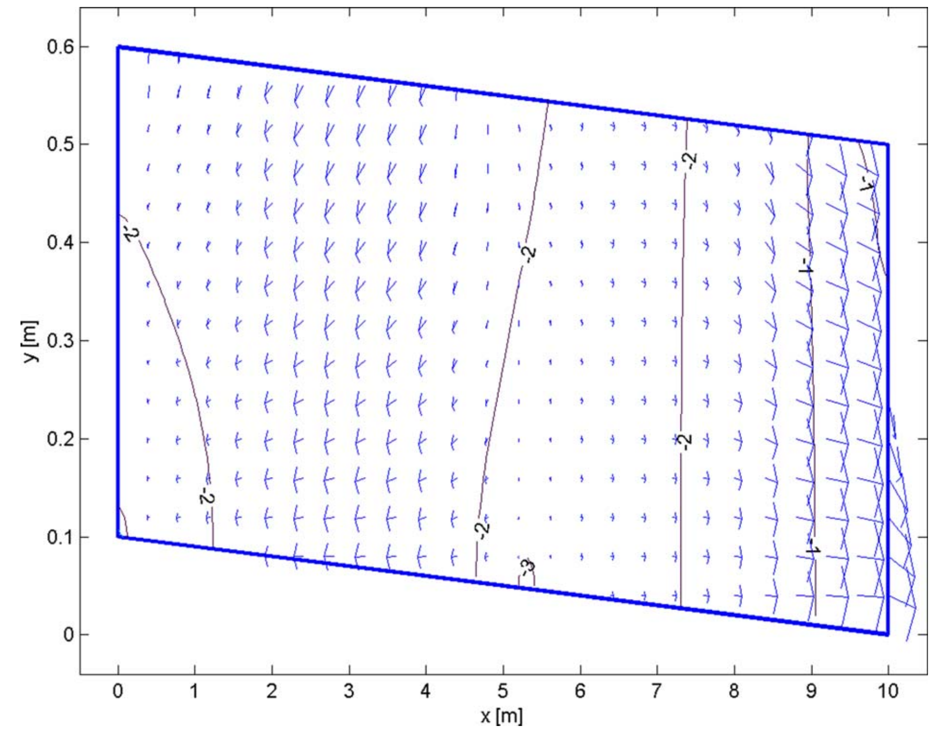

Figure 4 Specific-discharge vectors at $t = 1750$ s. The length of the vector is proportional to the ten-based logarithm of its magnitude, measured in mh^{-1}. The contour-line values correspond to magnitudes of 0.1, 0.01, and 0.001 mh^{-1}, respectively.

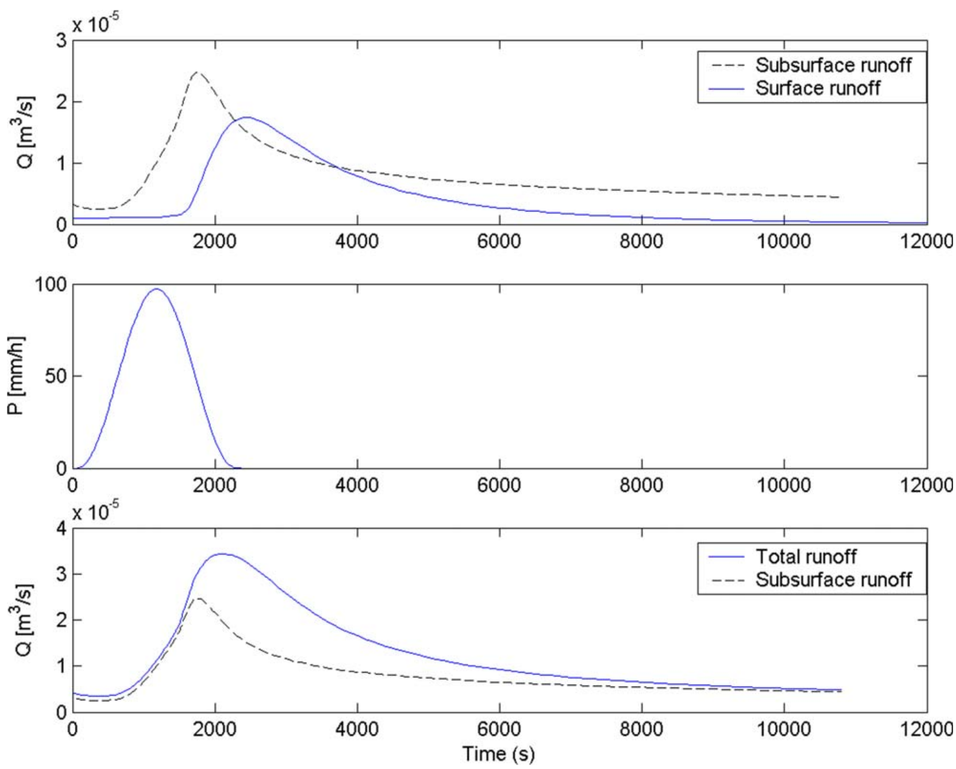

Figure 5 Rainfall hyetograph and the resulting surface, subsurface, and total runoff hydrographs of a completely horizontal aquifer.

If, on the other hand, groundwater ridging is defined as the formation of a high-pressure subsurface ridge along the stream, coupled with relatively steep hydraulic head gradients on both sides (but especially on the stream side) of the ridge, then groundwater ridging seems to be connected to the observed fast baseflow response to the stream. Figs. 2 and 3 suggest that the release of groundwater to the stream is proportional to this groundwater mounding. A cause and effect relationship between rapid baseflow response and a high pressure ridge next to the stream, however, is absent. This can be proved by having a look at Fig. 5 where the runoff hydrographs of a com-

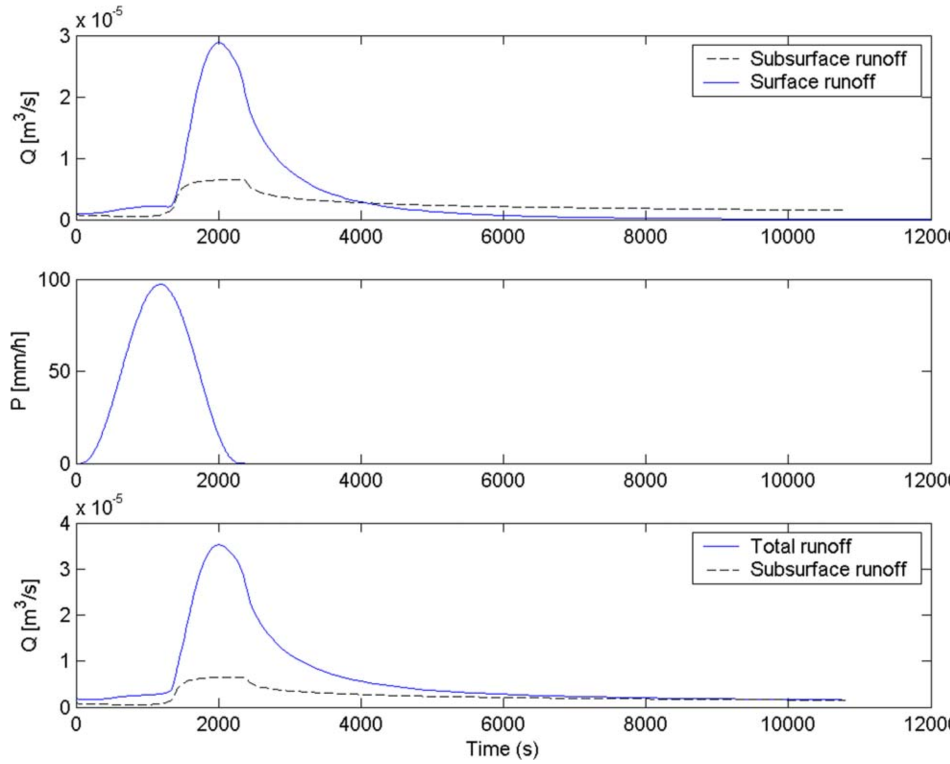

Figure 6 Rainfall hyetograph and the resulting surface, subsurface, and total runoff hydrographs of the gently sloping aquifer with reduced hydraulic conductivity values.

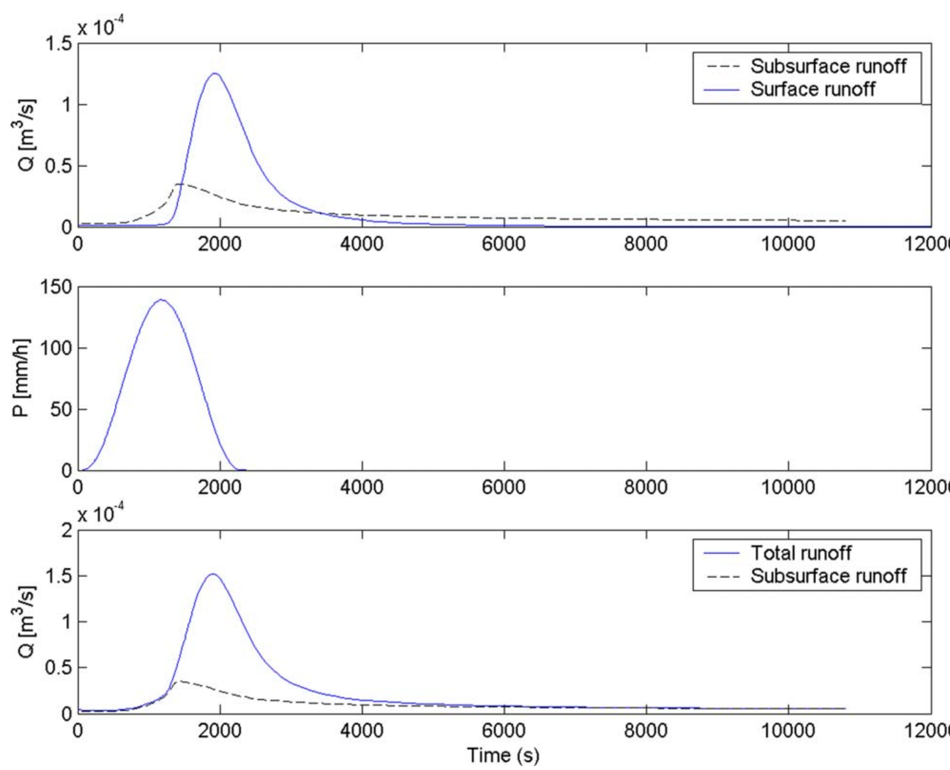

Figure 7 Rainfall hyetograph and the resulting surface, subsurface, and total runoff hydrographs of the gently sloping aquifer.

pletely horizontal aquifer with zero ground surface and impermeable layer slopes are displayed. Here the groundwater initially is the same distance from the surface along the aquifer, thus no groundwater ridging through time will occur alongside the stream. Instead, the groundwater table follows a typical drawdown curve at all $t > 0$ times. Yet, the subsurface runoff hydrograph is very similar (both in volume and timing of its peak) to the previous gently sloping surface and impermeable layer case (Fig. 3). Moreover the baseflow peak now is even higher somewhat than with groundwater ridging. The only plausible explanation is that ridging is not the cause of fast and abundant baseflow contribution to the stream, rather, the sharp hydraulic gradient condition necessarily developing next to the stream is. Groundwater ridging even counteracts to a certain degree the draining effect of the overall head gradients in the aquifer by diverting water away from the stream for some time, as seen in Fig. 4 and discussed by Cloke et al. (2006), resulting in a slightly diminished baseflow peak as evidenced by the comparison of Figs. 3 and 5. (As a side note, for the separate surface runoff calculations (and only there) a slope of 0.1% was employed in this completely horizontal aquifer case in order to obtain any surface runoff response. Also of secondary importance is the fact that in the completely horizontal aquifer case the total runoff volume is larger in the approx. 3-h interval than with the sloping aquifer. This is so because the initial water content of the horizontal aquifer is larger than that of the latter.)

I would also like to point out that the presence of a high pressure subsurface ridge in itself is not indicative (even if not as a cause and effect) of a potential rapid baseflow response in cases where the hydraulic conductivity of the soil-aquifer system is not sufficient enough. This is exemplified in Fig. 6, where the gently sloping aquifer is subjected to the same conditions as previously with the only exception that the hydraulic conductivity values (as a function of ψ) were reduced by a factor of ten. The resulting baseflow response is not only diminished in volume but also delayed in time. This underlines the potential importance of preferential flow in rapid groundwater response.

As a final note, I would also add that the relative volume of the baseflow response to total runoff of the aquifer in the present experiment is further influenced by the intensity (and/or duration) of the precipitation event (Fig. 7). Moreover, precipitation intensity has an effect on the timing of the baseflow peak as well (compare Figs. 3 and 7), since higher infiltration rates can saturate the soil (and build up sharp hydraulic head gradients) faster.

References

Abdul, A.S., Gillham, R.W., 1984. Laboratory studies of the effects of the capillary fringe on streamflow generation. Water Resources Research 20, 691–698.

Berod, D.D., Singh, V.P., Musy, A., 1999. A geomorphologic kinematic-wave (GKW) model for estimation of floods from small alpine watersheds. Hydrological Processes 13, 1391–1416.

Cloke, H.L., Anderson, M.G., McDonnell, J.J., Renaud, J.-P., 2006. Using numerical modelling to evaluate the capillary fringe groundwater ridging hypothesis of streamflow generation. Journal of Hydrology 316, 141–162.

Gitirana, G. Jr., Fredlund, M.D., Fredlund, D.G., 2005. Infiltration-runoff boundary conditions in seepage analysis. In: 58th Canadian Geotechnical Conference and 6th Joint IAH-CGS Conference, September 19–21, Saskatchewan, Canada.

Lam, L., Fredlund, D.G., Barbour, S.L., 1987. Transient seepage model for saturated-unsaturated soil systems: A geotechnical engineering approach. Canadian Geotechnical Journal 24, 565–580.

Szilagyi, J., 2003. Sensitivity analysis of aquifer parameter estimations based on the Laplace equation with linearized boundary conditions. Water Resources Research 3 (6), 1156.